

## Research Article

# Examination of Machining Parameters and Prediction of Cutting Velocity and Surface Roughness Using RSM and ANN Using WEDM of Altemp HX

I. V. Manoj <sup>1</sup>, Hargovind Soni <sup>2</sup>, S. Narendranath <sup>1</sup>, P. M. Mashinini,<sup>2</sup> and Fuat Kara <sup>3</sup>

<sup>1</sup>Department of Mechanical Engineering, National Institute of Technology Karnataka, Surathkal 575025, India

<sup>2</sup>Department of Mechanical and Industrial Engineering Technology, University of Johannesburg, Johannesburg, South Africa

<sup>3</sup>Düzce University Engineering, Faculty Department of Mechanical Engineering, Düzce, Turkey

Correspondence should be addressed to Hargovind Soni; hargovindsoni2002@gmail.com and Fuat Kara; fuatkara@duzce.edu.tr

Received 16 August 2021; Accepted 8 January 2022; Published 18 January 2022

Academic Editor: Alicia E. Ares

Copyright © 2022 I. V. Manoj et al. This is an open access article distributed under the Creative Commons Attribution License, which permits unrestricted use, distribution, and reproduction in any medium, provided the original work is properly cited.

The Altemp HX is a nickel-based superalloy having many applications in chemical, nuclear, aerospace, and marine industries. Machining such superalloys is challenging as it may cause both tool and surface damage. WEDM, a non-contact machining technique, can be employed in the machining of such alloys. In the present study, different input parameters which include pulse on time, wire span, and servo gap voltage were investigated. The cutting velocity, surface roughness, recast layer, and microhardness variations were examined on the WEDMed surface. The genetic algorithm was used to optimize the cutting velocity and surface roughness, thereby improving the overall quality of the product. The highest recast layer values were recorded as 25.8  $\mu\text{m}$ , and the lowest microhardness was 170 HV. Response surface methodology and artificial neural network were employed for the prediction of cutting velocity and surface roughness. Artificial neural network prediction technique was the most efficient method for the prediction of response parameters as it predicted an error percentage lesser than 6%.

## 1. Introduction

Altemp HX is a high-temperature and high-strength superalloy having many applications. It can be used in spray bars, flame holders, tailpipes, turbines, propellers, furnaces, etc. WEDM technology is established as a feasible alternate solution for the machining of such critical aerospace components made of superalloys. Many researchers have machined different nickel-based alloys using WEDM [1–3]. Majumder et al. [4] stated that in WEDM of Inconel 800, there was a requirement of a tradeoff between cutting time and surface roughness for obtaining good quality components. Different researchers have tried different optimization methods for increasing productivity [5–8]. Kumar et al. [9] investigated surface crack density and recast layer thickness using response surface methodology. The parameters such as pulse on time, peak current, and pulse off time influenced most on surface crack density, and recast layer thickness was

influenced by pulse on time. Singh and Pradhan [10] explored the parametric effects by using the Taguchi technique and Response Surface Methodology (RSM) in WEDM of AISI D2 Steel. The parameters such as material removal rate and the surface roughness were minimized in optimal settings of machining parameters. Singh et al. [11] optimized WEDM parameters such as MRR and Kerf width using the multiresponse function of the RSM technique. It was found that the peak current, gap voltage, and duty cycle are the major parameters that affect material removal rate and kerf width. Bose and Nandi [12] have investigated and optimized material removal rate (MRR), surface roughness (SR), kerf width, and overcut using RSM. Different parametric effects on the output parameters were analyzed and optimized. Varun and Venkaiah [13] have proposed grey relational analysis with a genetic algorithm to simultaneously optimize the response parameters such as material removal rate, surface roughness, and cutting width (kerf). Altug et al. [14]

have machined Ti6Al4V in WEDM with different heat treatments, and the effect of machining parameters was analyzed. It was observed that the optimization of output parameters using a genetic algorithm yielded minimum kerf. Kumar et al. [15] have employed response surface methodology center composite second-order rotatable design for designing the experiments, and a genetic algorithm has been used for the optimization of the surface finish of the machined surface in Wire EDM. Sharma et al. [16] conducted an RSM-based overcut model using a genetic algorithm for finding optimal machining parameters. This method was also used for the prediction as the error between the predicted and experimental values lies in the range of  $\pm 10\%$ . Goyal et al. [17] have investigated an integrated approach of nondominated sorting genetic algorithm-II for multi-objective optimization of MRR and WWR, where errors were less than 10%.

Soni et al. [18] used the response surface method and ANN for the prediction of cutting speed in WEDM of shape memory alloys. Manoj and Narendranath [19, 20] have used ANN for the prediction of profile areas and profiling speed. It was concluded that both machining parameters and taper angle influence the accuracy and profiling speed. Phate and Toney [21] have predicted the surface roughness and material removal rate using ANN and dimensional analysis models where the ANN model proved to be the most accurate. Ming et al. [22] have reported ANN using BPNN with the mean squared error that was suitable in the prediction of surface roughness and material removal rate. Chou et al. [23] have also reported the prediction of real-time predict wire rupture, and the prediction accuracy of wire rupture was reported above 85% using ANN.

The literature shows the importance of machining parameters on the efficiency of machining. In the present investigation, Altemp HX, a nickel-based superalloy, was machined in WEDM. Different input parameters such as pulse on time, wire span, and servo gap voltage on cutting velocity, surface roughness, recast layer, and microhardness were examined on the machined surface.

## 2. Materials

Altemp HX is a wrought nickel base alloy having excellent oxidation resistance and superior high-temperature strength of up to 1200°C (2200°F). This alloy has high mechanical properties such as high resistance to stress-corrosion cracking, fabricability, low creep, and high-temperature strength. The received material was heat-treated at 1175°C (2150°F). The EDS of Altemp HX is shown in Figure 1, which shows the element's composition.

## 3. Experimental Particulars and Parametric Details

The wire electric discharge machine of 'ECOCUT ELPLUS 15' by Electronica machine tools was used. The zinc-coated copper wire was used to cut the nickel-based alloy. The workpiece is fixed to the WEDM table. Both the workpiece and electrode were maintained at high voltage. The

dielectric fluid always engulfed by the electrode. This leads to ionization due to which the spark is generated. The sparks melt the material, and the dielectric fluid carries the melted material as debris. Figure 2(a) shows the work material placed on the WEDM table. Figure 2(b) shows the specimens machined at different parameters. Table 1 shows the machining parameters that have been fixed by primary experiments. These parameters were selected based on initial experiments and machine capabilities. The input parameters were pulse on time, wire span, and servo gap voltage. Different effects of input parameters on output characteristics were analyzed.  $L_{25}$  Taguchi's orthogonal experiment was employed for the examination. Table 2 shows the parameters and their levels used for machining.

## 4. Results and Discussions

The cutting velocity and surface roughness were recorded at different parameters, as shown in Table 3. It can be observed that at the highest machining parameters, the cutting velocity was 2.455 mm/min and the surface roughness was 3.76  $\mu\text{m}$ , whereas at the lowest machining parameters, the cutting velocity was 0.504 mm/min with 1.33  $\mu\text{m}$  surface roughness. The surface roughness was calculated as an average of 5 values, and the cutting velocity was the average of all the machining speeds recorded at every instant of machining the material.

### 4.1. ANOVA and Effect Plots for Different Parameters.

Table 4 and Figure 3 show the analysis of variance and effect plots for cutting velocity and surface roughness, respectively. It can be noted that among all the parameters, pulse on time ( $T_{\text{on}}$ ) was the most contributing and significant factor. From the effect plots, as shown in Figures 3(a) and 3(b), it can be observed that as  $T_{\text{on}}$  increases, both cutting velocity and surface roughness increase.  $T_{\text{on}}$  influences the discharge energy. As  $T_{\text{on}}$  increases, the ionization occurring at the interface of the workpiece also increases. This increases the discharge energy, so the material melts faster. This increases the cutting velocity, as shown in Figure 3(a). In the case of surface roughness, at higher  $T_{\text{on}}$ , the ionization is higher. This increase in ionization increases spark generation intensity. With higher spark intensity, the craters formed on the WEDMed surface become deeper and larger. This increases the surface roughness of the machined surface. At lower  $T_{\text{on}}$ , the discharge energy decreases; this will reduce the melting of the material. This decreases the cutting velocity due to lower spark intensity. The craters formed on the WEDMed surface at lower spark intensity are smaller and shallower, resulting in lower surface roughness [24, 25].

The wire span (WS) is the distance of the wire between the upper and lower guide during machining. As the WS increases, the tension in the wire decreases which leads to an increase in wire vibration [26, 27]. This increase in wire vibration causes lower cutting velocity due to variation in spark gap [24, 28]. In the case of machining at lower WS, the wire tension is higher. This results in low wire vibration which avoids variation in spark gap [29]. So, the cutting

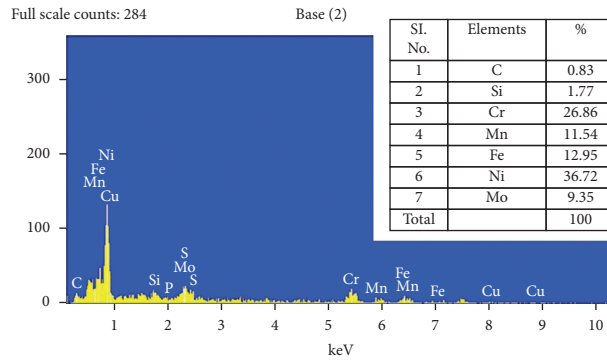


FIGURE 1: EDS of Altemp HX.

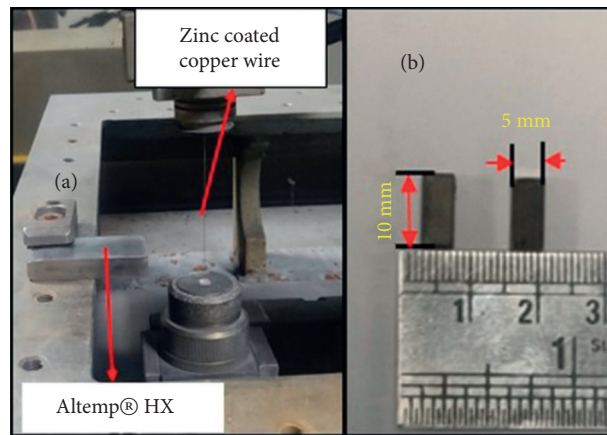


FIGURE 2: (a) Altemp HX fixed in WEDM table. (b) Workpieces machined at different parameters.

TABLE 1: Machining parameters.

Parameter	Specifications
Wire diameter (mm)	0.25
Wire material	Zinc coated copper wire
Dielectric fluid	Deionized water
Pulse on time ( $\mu$ s)	105, 110, 115, 120, 125
Servo gap voltage (V)	35, 40, 45, 50, 55
Wire span feed (m/min)	4
Servo feed (mm/min)	20
Pulse off time ( $\mu$ s)	33

TABLE 2: Experimental parameters used for investigation.

Parameter	Level 1	Level 2	Level 3	Level 4	Level 5
Pulse on time ( $\mu$ s) ( $T_{on}$ )	105	110	115	120	125
Wire span (mm) (WS)	60	90	120	150	180
Servo gap voltage (V) (SGV)	35	40	45	50	55

velocity is higher at lower WS, as shown in Figure 3(a). With lower wire tension, the surface roughness decreases as there is variation in the spark gap. This variation decreases the

spark intensity which leads to shallower and small craters [25]. Therefore, as the WS increases, the surface roughness decreases, as in Figure 3(b).

In the case of Servo gap voltage (SGV), as SGV increases, the spark gap between workpiece and wire also increases. This results in lower ionization which decreases the discharge energy and spark intensity. Therefore material melting time reduces leading to lower cutting velocity. The surface roughness decreases as the ionization is lower. This decreases spark intensity giving shallower and smaller craters decreasing the surface roughness. In the case of lower SGV, as the spark gap decreases the cutting velocity increases because of the increase in the spark intensity and discharge. Surface roughness also increases due to the formation of larger and deeper craters [25].

#### 4.2. Regression Equations by Response Surface Methodology.

For the parametric combinations in Table 3, the response surface method was employed using MINITAB. The equations (1) and (2) show the regression equations obtained by the response surface method used for optimization in the genetic algorithm. These equations show a mathematical relation of the parameters used in the investigation with the response characteristics.

TABLE 3: Response at different machining parameters.

Test no.	T <sub>on</sub> (μs)	WS (mm)	SGV (V)	CV (mm/min)	SR Ra (μm)
1	105	60	35	1.293	2.34
2	105	90	40	1.287	1.99
3	105	120	45	1.164	2.00
4	105	150	50	0.835	1.59
5	<b>105</b>	<b>180</b>	<b>55</b>	<b>0.504</b>	<b>1.33</b>
6	110	60	40	1.570	2.62
7	110	90	45	1.477	2.35
8	110	120	50	1.281	2.10
9	110	150	55	0.949	1.94
10	110	180	35	1.609	2.32
11	115	60	45	1.921	2.86
12	115	90	50	2.068	3.16
13	115	120	55	1.420	2.72
14	115	150	35	1.891	3.44
15	115	180	40	1.775	3.02
16	120	60	50	2.200	3.53
17	120	90	55	2.201	3.35
18	120	120	35	1.693	3.26
19	120	150	40	1.790	3.19
20	120	180	45	1.651	3.10
21	<b>125</b>	<b>60</b>	<b>55</b>	<b>2.455</b>	<b>3.76</b>
22	125	90	35	2.155	3.66
23	125	120	40	2.040	3.74
24	125	150	45	1.789	3.50
25	125	180	50	1.409	3.22

TABLE 4: ANOVA for cutting velocity and surface roughness.

Sl. no.	Parameters	DF	Adj. SS	Adj. MS	F value	P value	Contribution (%) contribution
Cutting velocity							
1	Pulse on time	4	3.328	0.832	14.4	0.001	63.45
2	Wire span	4	1.053	0.263	4.56	0.018	20.08
3	Servo gap voltage	4	0.170	0.042	0.74	0.584	3.25
4	Error	12	0.693	0.058			13.22
5	Total	24	5.245				
Surface roughness							
1	Pulse on time	4	10.392	2.598	70.07	0.001	87.49
2	Wire span	4	0.504	0.126	3.4	0.044	4.24
3	Servo gap voltage	4	0.537	0.134	3.62	0.037	4.52
4	Error	12	0.445	0.037			3.75
5	Total	24	11.878				

$$\begin{aligned}
 \text{cutting velocity} = & -32.14 + 0.582 T_{on} + 0.0748 WS - 0.2683 SGV \\
 & - 0.002693 T_{on} * T_{on} - 0.000031 WS * WS - 0.001791 SGV * SGV - 0.000613 T_{on} * WS + 0.003555 T_{on} * SGV,
 \end{aligned}
 \tag{1}$$

$$\begin{aligned}
 \text{surface roughness} = & -28.4 + 0.538 T_{on} + 0.0204 WS - 0.234 SGV - 0.002264 T_{on} * T_{on} \\
 & - 0.000026 WS * WS - 0.00020 SGV * SGV - 0.000145 T_{on} * WS + 0.00199 T_{on} * SGV.
 \end{aligned}
 \tag{2}$$

4.3. Genetic Algorithm. The genetic algorithm (GA) method is based on genetics and natural selection. It is employed to find optimal or near-optimal solutions to difficult problems. It works on three types of operators, namely, reproduction, crossover, and mutation. The strongest pair was chosen, and mutation was introduced due to the different crossovers in the gene pool. The strongest and best among them is chosen

as solutions [14]. In the case of the above investigation, the cutting velocity and surface roughness must be optimized by making a tradeoff to maintain the quality of the product. The optimization is carried out in the GA Toolbox of MATLAB environment with parameters, as shown in Table 5. It was seen that 105 (T<sub>on</sub>), 81(WS), and 53(SGV) were the optimal parameters. The boundary conditions were fed to the

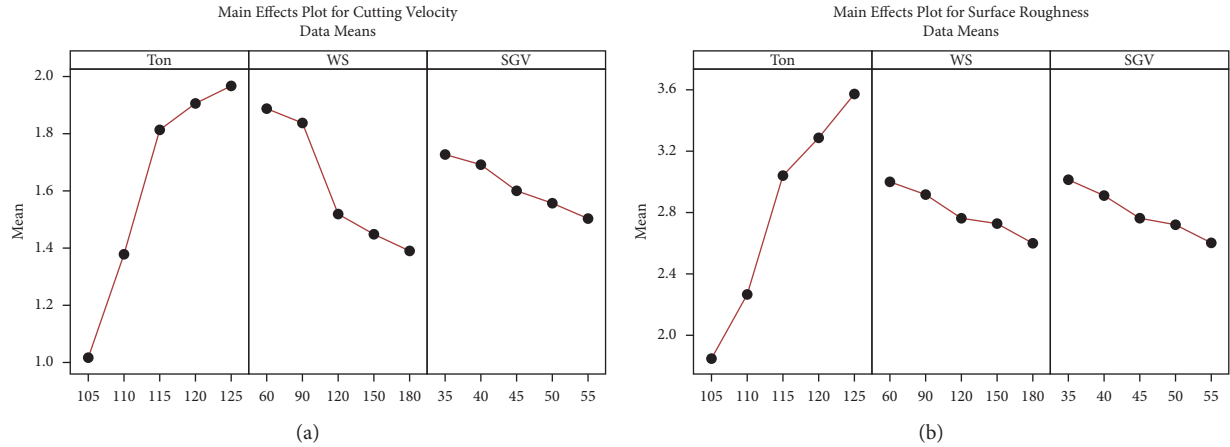


FIGURE 3: Variation of (a) cutting velocity and (b) surface roughness.

MATLAB software based on the parameters that were chosen for the machining. These parameters were derived from initial experiments. The below conditions are given for the genetic algorithm optimization with the help of equations (3)–(5):

$$110 \leq T_{ON} \leq 125; \quad (3)$$

$$60 \leq WS \leq 180; \quad (4)$$

$$35 \leq SGV \leq 55. \quad (5)$$

**4.4. Recast Layer Thickness and Micro-Hardness.** Figure 4 shows the recast layer formed on the WEDMed surface for the highest and lowest machining parameters. During machining, the temperature increases in the machining zone due to the discharge energy. This melts the material, and the molten metal is cooled by the dielectric fluid. This resolidifies, and a part of it is carried away as debris, and the other part forms as the recast layer at the top of the machined surface. At higher discharge energy, the melting of the material increases. This escalates the molten metal that was formed on the WEDMed surface. Therefore, with the increase in discharge energy, the recast layer thickness increases. The highest machining parameter generates the maximum discharge energy with the highest recast layer thickness, as shown in Figure 4. Figure 4(a) indicates the highest average recast layer thickness, i.e.,  $25.8 \mu\text{m}$  was measured at the highest cutting rate. The lowest machining parameters produced minimum average recast layer thickness, i.e.,  $7.6 \mu\text{m}$  due to minimal discharge energy, as shown in Figure 4(b). This causes thermal degradation on the WEDMed surface due to melting and cooling during machining. A comparable phenomenon was highlighted by Sharma et al. [24] during the WEDM of Inconel 706. This is further validated by the microhardness of the machined surface, as shown in Figure 5. It can be seen that the highest machining parameters have the lowest hardness of 166 HV, and the lowest machining parameter has the highest

hardness of 176 HV. This phenomenon was witnessed because at the highest parameters, the heat generated is maximum. This results in a higher temperature at the machining zone. The material melts and resolidifies due to the influence of cooling by dielectric fluid. This leads to a change in the properties of the hardness of the WEDMed surface. Similar results have been observed by Soni et al. [30] and Joy et al. [31].

**4.5. Prediction of Response Parameters Using RSM and ANN Methods.** The cutting velocity and surface roughness were predicted for different parameters using response surface methodology and an artificial neural network.

**4.5.1. Response Surface Methodology.** The response surface methodology is used for designing the experiments, fitting or formulating a model, optimization, and prediction. The output response in response surface methodology is given by the following equation [32]:

$$M = \alpha_0 + \sum_{x=1}^k \alpha_x p_x + \sum_{x=1}^k \alpha_{xx} p_x^2 + \sum_{x,y=1, x \neq y}^k \alpha_{xy} p_x p_y + \vartheta, \quad (6)$$

where  $\vartheta$  is the noise or error that is observed in the response  $M$ .  $p_x$  is the linear input variables,  $p_x^2$  and  $p_x p_y$  are the squares and interaction terms, respectively, of these input variables. The unknown second-order regression coefficients  $\alpha_0, \alpha_x, \alpha_{xx}, \alpha_{xy}$ , which should be determined in the second-order model, are obtained by the least square method.

**4.5.2. Artificial Neural Network.** The artificial neural network was used for the prediction of cutting velocity and surface roughness. The ANN mimics some basic aspects of brain functions. It works on neuron weights, inputs, activation function, summation function, and output [33, 34]. The optimal model was trained in the MATLAB platform by the ANN toolbox. Different iterations were used having various parametric combinations for training (15 experiments), validation (5 experiments), and testing

TABLE 5: Genetic algorithm optimization parameters.

Sl. no.	Pulse on time ( $T_{on}$ )	Wire span (WS)	Servo gap voltage (SGV)	Cutting velocity (mm/min)		Surface roughness ( $\mu\text{m}$ )	
				Experimental	Optimum	Experimental	Optimum
1	105	81	53	0.54	0.501	1.52	1.566

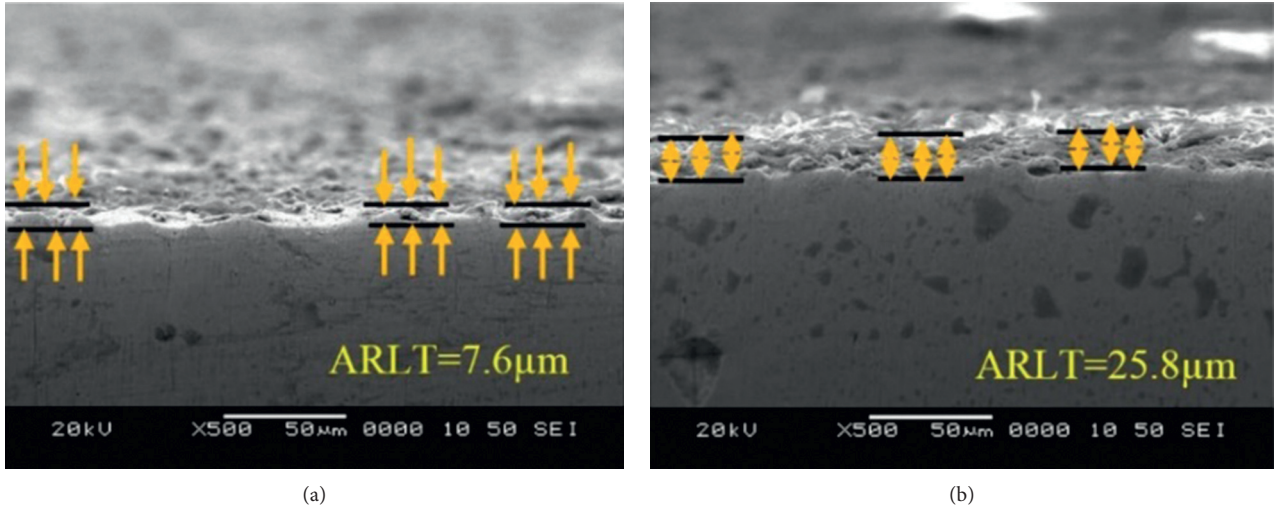


FIGURE 4: SEM images of WEDMed surface. (a) Lowest machining parameter. (b) Highest machining parameter.

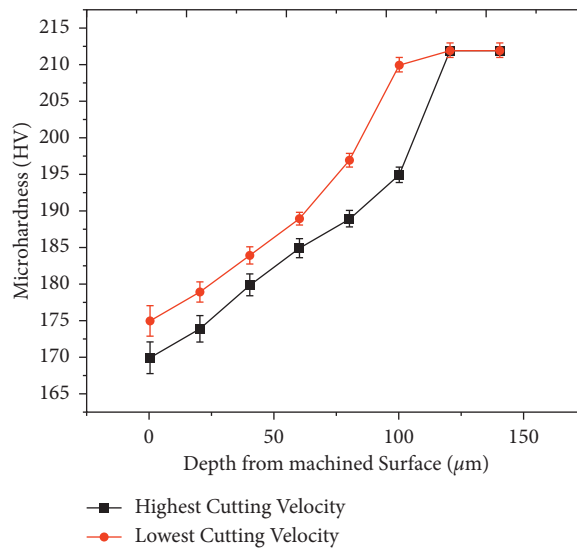


FIGURE 5: Variation of microhardness at different cutting velocities.

(5 experiments). The network structure with 3-5-1-1 was used for the prediction of both cutting velocity and surface roughness. Log-sigmoid and pureline functions were employed for the prediction using a feedforward neural network. Table 6 shows different predictions for cutting

velocity and surface roughness using ANN and RSM methods. It can be seen that ANN predictions have an error percentage lesser than 6%, whereas the RSM predictions yielded an error percentage ranging from 0.58 to 13.95%.

TABLE 6: Prediction of cutting velocity and surface roughness by RSM and ANN.

Sl. no	Experimental value	RSM prediction	Error (%)	ANN prediction	Error (%)
<i>CV (mm/min)</i>					
1	1.293	1.24	4.28	1.28	0.94
2	1.287	1.26	2.15	1.30	1.34
3	1.164	1.14	1.99	1.15	1.39
4	0.835	0.88	4.76	0.87	4.08
5	0.504	0.47	8.15	0.50	0.17
6	1.57	1.63	3.43	1.62	3.31
7	1.477	1.56	5.36	1.48	0.08
8	1.281	1.35	5.07	1.28	0.08
9	0.949	0.99	4.35	0.94	0.43
10	1.609	1.68	4.01	1.64	1.82
11	1.921	1.97	2.61	1.92	0.03
12	2.068	1.81	13.95	1.99	3.77
13	1.42	1.51	6.02	1.46	2.78
14	1.891	1.80	4.82	1.89	0.07
15	1.775	1.66	7.17	1.82	2.32
16	2.2	2.27	3.20	2.20	0.02
17	2.201	2.02	8.83	2.21	0.42
18	1.693	1.92	12.04	1.72	1.67
19	1.79	1.83	2.20	1.77	0.91
20	1.651	1.59	3.86	1.64	0.48
21	2.455	2.53	2.84	2.45	0.15
22	2.155	2.04	5.74	2.17	0.93
23	2.04	2.00	2.16	1.99	2.23
24	1.789	1.81	1.15	1.81	1.38
25	1.409	1.48	4.58	1.41	0.24
<i>SR (<math>\mu\text{m}</math>)</i>					
1	2.34	2.23	4.84	2.45	4.70
2	1.99	2.07	3.90	1.99	0.06
3	2.00	1.85	7.38	2.11	5.50
4	1.59	1.58	0.58	1.61	1.26
5	1.33	1.25	5.83	1.35	1.50
6	2.62	2.64	0.71	2.68	2.29
7	2.35	2.50	6.29	2.44	3.83
8	2.1	2.30	9.55	2.20	4.76
9	1.94	2.05	5.52	1.96	1.03
10	2.32	2.58	11.09	2.36	1.72
11	2.86	3.03	5.83	2.90	1.40
12	3.16	2.90	8.09	3.19	0.95
13	2.72	2.73	0.19	2.78	2.10
14	3.44	3.08	10.42	3.45	0.29
15	3.02	2.84	6.00	3.11	2.98
16	3.53	3.39	3.92	3.60	1.98
17	3.35	3.29	1.88	3.40	1.49
18	3.26	3.47	6.42	3.28	0.61
19	3.19	3.30	3.49	3.17	0.63
20	3.1	3.08	0.75	3.11	0.32
21	3.66	3.73	1.99	3.72	1.64
22	3.76	3.74	0.52	3.76	0.00
23	3.74	3.65	2.48	3.71	0.80
24	3.5	3.56	1.71	3.49	0.29
25	3.22	3.29	2.21	3.22	0.07

## 5. Conclusions

From the above study, Altemp HX, a nickel superalloy, was machined at different levels, and the effect of machining parameters was analyzed. It was noticed that WS and SGV decrease both response parameters, but an escalation in

pulse on time increased both cutting velocity and surface roughness.  $T_{on}$  was the most influential and contributing factors on response parameters. The genetic algorithm was used for the optimization of cutting velocity and surface roughness. It was observed that the experimental values were in coordination with optimized responses, and the

percentage deviation was less than 3%. RSM and ANN were used for prediction, and it was observed that the ANN was most accurate, and it predicted a percentage error ranging between 0–6 percent.

## Data Availability

The data used to support the findings of this study are available from the corresponding author or within the article upon request.

## Conflicts of Interest

The authors declare that they have no conflicts of interest.

## References

- [1] M. T. Antar, S. L. Soo, D. K. Aspinwall et al., "Fatigue response of Udimet 720 following minimum damage wire electrical discharge machining," *Materials & Design*, vol. 42, pp. 295–300, 2012.
- [2] I. V. Manoj and S. Narendranath, "Wire electric discharge machining at different slant angles during slant type taper profiling of microfer 4722 superalloy," *Journal of Materials Engineering and Performance*, vol. 31, pp. 697–708, 2021.
- [3] V. K. Rohilla, R. Goyal, A. Kumar, Y. K. Singla, and N. Sharma, "Surface integrity analysis of surfaces of nickel-based alloys machined with distilled water and aluminium powder-mixed dielectric fluid after WEDM," *International Journal of Advanced Manufacturing Technology*, vol. 116, no. 7-8, pp. 2467–2472, 2021.
- [4] H. Majumder, T. R. Paul, V. Dey, P. Dutta, and A. Saha, "Use of PCA-grey analysis and RSM to model cutting time and surface finish of Inconel 800 during wire electro discharge cutting," *Measurement*, vol. 107, pp. 19–30, 2017.
- [5] H. Soni, S. Narendranath, and M. R. Ramesh, "Effect of machining parameters on wire electro discharge machining of shape memory alloys analyzed using grey entropy method," *Journal of Material Science and Mechanical Engineering*, vol. 2, no. 13, pp. 50–54, 2015.
- [6] F. Kara and A. Takmaz, "Optimization of cryogenic treatment effects on the surface roughness of cutting tools," *Materials Testing*, vol. 61, no. 11, pp. 1101–1104, 2019.
- [7] F. Kara, U. Köklü, and U. Kabasakaloğlu, "Taguchi optimization of surface roughness in grinding of cryogenically treated AISI 5140 steel," *Materials Testing*, vol. 62, no. 10, pp. 1041–1047, 2020.
- [8] B. Öztürk and F. Kara, "Calculation and estimation of surface roughness and energy consumption in milling of 6061 alloy," *Advances in Materials Science and Engineering*, vol. 2020, Article ID 5687951, 12 pages, 2020.
- [9] A. Kumar, V. Kumar, and J. Kumar, "Surface crack density and recast layer thickness analysis in WEDM process through response surface methodology," *Machining Science and Technology*, vol. 20, no. 2, pp. 201–230, 2016.
- [10] V. Singh and S. K. Pradhan, "Optimization of WEDM parameters using Taguchi technique and response surface methodology in machining of AISI D2 steel," *Procedia Engineering*, vol. 97, pp. 1597–1608, 2014.
- [11] B. P. Singh, J. Singh, J. Singh, M. bhayana, and D. Goyal, "Experimental Investigation of Machining nimonic-80A alloy on Wire EDM Using Response Surface Methodology," *Metal Powder Report*, 2021, In press.
- [12] S. Bose and T. Nandi, "Measurement of performance parameters and improvement in optimized solution of WEDM on a novel titanium hybrid composite," *Measurement*, vol. 171, pp. 1–16, 2021.
- [13] A. Varun and N. Venkaiah, "Simultaneous optimization of WEDM responses using grey relational analysis coupled with genetic algorithm while machining EN 353," *International Journal of Advanced Manufacturing Technology*, vol. 76, no. 1-4, pp. 675–690, 2015.
- [14] M. Altug, M. Erdem, and C. Ozay, "Experimental investigation of kerf of Ti6Al4V exposed to different heat treatment processes in WEDM and optimization of parameters using genetic algorithm," *International Journal of Advanced Manufacturing Technology*, vol. 78, no. 9-12, pp. 1573–1583, 2015.
- [15] P. M. Kumar, D. Dinesh, G. Sundararaju, S. Madheswaran, and K. Perumal, "Modelling of surface roughness in wire-EDM using response surface methodology technique," *Advances in Materials Research. Springer Proceedings in Materials*, Springer, vol. 5, Singapore, , 2021.
- [16] N. Sharma, R. Khanna, and R. D. Gupta, "WEDM process variables investigation for HSLA by response surface methodology and genetic algorithm," *Engineering Science and Technology, an International Journal*, vol. 18, no. 2, pp. 171–177, 2015.
- [17] A. Goyal, N. Gautam, and V. K. Pathak, "An adaptive neuro-fuzzy and NSGA-II-based hybrid approach for modelling and multi-objective optimization of WEDM quality characteristics during machining titanium alloy," *Neural Computing & Applications*, vol. 33, no. 23, pp. 16659–16674, 2021.
- [18] H. Soni, S. Narendranath, and M. R. Ramesh, "ANN and RSM modeling methods for predicting material removal rate and surface roughness during WEDM of Ti50Ni40Co10 shape memory alloy," *AMSE Journals-Amse Iieta*, vol. 54, no. 3, pp. 435–444, 2017.
- [19] I. V. Manoj and S. Narendranath, "Machining and forecasting of square profile areas using artificial neural modelling at different slant angles by WEDM," *IOP Conference Series: Materials Science and Engineering*, vol. 1065, pp. 1–7, 2021.
- [20] I. Manoj and S. Narendranath, "Variation and artificial neural network prediction of profile areas during slant type taper profiling of triangle at different machining parameters on Hastelloy X by wire electric discharge machining," *Proceedings of the Institution of Mechanical Engineers - Part E: Journal of Process Mechanical Engineering*, vol. 234, no. 6, pp. 673–683, 2020.
- [21] M. R. Phate and S. B. Toney, "Modeling and prediction of WEDM performance parameters for Al/SiCp MMC using dimensional analysis and artificial neural network," *Engineering Science and Technology, an International Journal*, vol. 22, no. 2, pp. 468–476, 2019.
- [22] W. Ming, J. Hou, Z. Zhang et al., "Integrated ANN-LWPA for cutting parameter optimization in WEDM," *International Journal of Advanced Manufacturing Technology*, vol. 84, pp. 1277–1294, 2016.
- [23] P. H. Chou, Y. R. Hwang, and B. H. Yan, "The study of machine learning for wire rupture prediction in WEDM," *International Journal of Advanced Manufacturing Technology*, 2021.
- [24] P. Sharma, D. Chakradhar, and S. Narendranath, "Evaluation of WEDM performance characteristics of Inconel 706 for turbine disk application," *Materials & Design*, vol. 88, pp. 558–566, 2015.

- [25] V. Kumar, V. Kumar, and K. K. Jangra, "An experimental analysis and optimization of machining rate and surface characteristics in WEDM of Monel-400 using RSM and desirability approach," *Journal of Industrial Engineering International*, vol. 11, no. 3, pp. 297–307, 2015.
- [26] A. B. Puri and B. Bhattacharyya, "Modelling and analysis of the wire-tool vibration in wire-cut EDM," *Journal of Materials Processing Technology*, vol. 141, no. 3, pp. 295–301, 2003.
- [27] S. Habib and A. Okada, "Study on the movement of wire electrode during fine wire electrical discharge machining process," *Journal of Materials Processing Technology*, vol. 227, pp. 147–152, 2016.
- [28] T. Chaudhary, A. N. Siddiquee, and A. K. Chanda, "Effect of wire tension on different output responses during wire electric discharge machining on AISI 304 stainless steel," *Defence Technology*, vol. 15, no. 4, pp. 541–544, 2019.
- [29] S. Habib, "Optimization of machining parameters and wire vibration in wire electrical discharge machining process," *Mechanics of Advanced Materials and Modern Processes*, vol. 3, no. 1, pp. 1–9, 2017.
- [30] H. Soni, S. Narendranath, and M. R. Ramesh, "Effects of wire electro-discharge machining process parameters on the machined surface of Ti50Ni49Co1 shape memory alloy," *Silicon*, vol. 11, no. 2, pp. 733–739, 2019.
- [31] R. Joy, I. V. Manoj, and S. Narendranath, "Investigation of cutting speed, recast layer and micro-hardness in angular machining using slant type taper fixture by WEDM of Hastelloy X," *Materials Today Proceedings*, vol. 27, pp. 1943–1946, 2019.
- [32] S. K. Majhi, M. K. Pradhan, and H. Soni, "Optimization of EDM parameters using integrated approach of RSM, GRA and ENTROPY method," *International Journal of Applied Research in Mechanical Engineering*, vol. 3, no. 1, pp. 82–87, 2013.
- [33] A. Eser, E. A. Ayyıldız, M. Ayyıldız, and F. Kara, "Artificial intelligence-based surface roughness estimation modelling for milling of AA6061 alloy," *Hindawi Advances in Materials Science and Engineering*, vol. 2021, Article ID 5576600, 10 pages, 2021.
- [34] Y. Ö. Özgören, S. Çetinkaya, S. Sarıdemir, A. Çiçek, and F. Kara, "Artificial neural network based modelling of performance of a beta-type Stirling engine," *Proceedings of the Institution of Mechanical Engineers - Part E: Journal of Process Mechanical Engineering*, vol. 227, pp. 166–177, 2013.